International Journal of Rock Mechanics & Mining Sciences 48 (2011) 616–625

Contents lists available at ScienceDirect

International Journal of Rock Mechanics & Mining Sciences

journal homepage: www.elsevier.com/locate/ijrmms

Correlations between mining and seismicity for re-entry protocol development

J.A. Vallejos [a,b,*], S.D. McKinnon [a]

[a] Robert M. Buchan Department of Mining, Goodwin Hall, 25 Union Street, Queen's University, Kingston, Canada ON K7L 3N6
[b] Department of Mining Engineering, University of Chile, Santiago, Chile

ARTICLE INFO

Article history:
Received 25 May 2010
Received in revised form
30 December 2010
Accepted 12 February 2011
Available online 31 March 2011

Keywords:
Mining seismicity
Rockbursts
Seismic sequences
Re-entry protocol
Mine safety
Ground control

ABSTRACT

Re-entry protocols are a strategic approach for controlling risk after large magnitude events or blasts in seismically active mines by monitoring the return of seismicity to background levels. Restricting access to areas of a mine affected by seismicity for sufficient time to allow this decay to occur is the main approach in most re-entry protocols. In the present study mining and seismicity are correlated for re-entry protocol development by using a uniform statistical technique for the identification of background levels. The relations are established relying on a theoretical framework that links the productivity of seismicity with the decay time of seismic sequences. Three case histories are presented and analyzed, selected to illustrate the possible effects of factors, such as: volume of mined rock, depth, and magnitude of large events, on the decay time of mining-induced seismic sequences. Positive significant correlations between the decay time and the mining factors studied here are found.

1. Introduction

Immediately following large seismic events/rockburst or blasts in seismically active mines, there is a short-term increase in levels of seismicity, which gradually decays to background levels. During this time of elevated seismicity the risk of seismic events with sufficiently high magnitude to cause damage is also high and therefore the policy adopted by mines is to restrict access to the affected areas for a time period (space–time exclusion zone). This is the re-entry protocol.

In mines, the decay period is generally a matter of hours, but at the crustal scale, aftershocks can continue over months or years following the main event. This decay phenomenon is referred to as the modified Omori's law [1–3], which can be viewed as a complex relaxation processes occurring after a main event [4].

Based on a survey of current re-entry practices at 18 seismically active mines [5], generally, the decision to re-enter an affected area is based on the requirement for the rate of the monitored seismic parameter to return to a previously defined background level for a specified time window. If the rate exceeds the pre-set threshold during that time, the re-entry restriction continues. Fig. 1 illustrates these concepts for the event count parameter after a 2.4M_n (Nuttli scale) rockburst at the Copper Cliff North Mine. At each time t after the main event, the rate is calculated by performing a linear regression on the cumulative seismic parameter (Fig. 1b) using the data from a retrospective time window tw, the process being repeated at successive times by using a time shift ts. In Fig. 1c a 2 h time window with a 0.1 h shift was used to evaluate the seismicity rate. Re-entry is defined at the first point in the seismic sequence where the rate of the monitored seismic quantity is comparable to or lower than background levels.

The definition of when mining seismicity will be at background levels can be a challenging process for the development of re-entry protocols [6]. Based on the results of the survey, most mines have identified, at a basic level, typical background levels for re-entry protocol development.

The primary purpose of this paper is to establish statistical correlations between mining factors and the decay time of mining-induced seismic sequences. To accomplish this we have first developed a method for estimating background levels of seismicity rate for re-entry protocol development in connection with current re-entry practices. We then show a theoretical framework that links the productivity of seismicity with the decay time of seismic sequences. Finally, the method developed for estimating background levels of seismicity is applied to several case histories and used to correlate the decay time after blast and large magnitude events with mining factors, such as: volume of mined rock, depth and magnitude of the main event.

* Corresponding author at: Robert M. Buchan Department of Mining, Goodwin Hall, 25 Union Street, Kingston, ON Canada K7L 3N6.
Tel.: +613 533 2230; fax: +613 533 6597.
E-mail addresses: javier.vallejos@mine.queensu.ca (J.A. Vallejos), sm@mine.queensu.ca (S.D. McKinnon).

1365-1609/$ - see front matter © 2011 Elsevier Ltd. All rights reserved.
doi:10.1016/j.ijrmms.2011.02.014

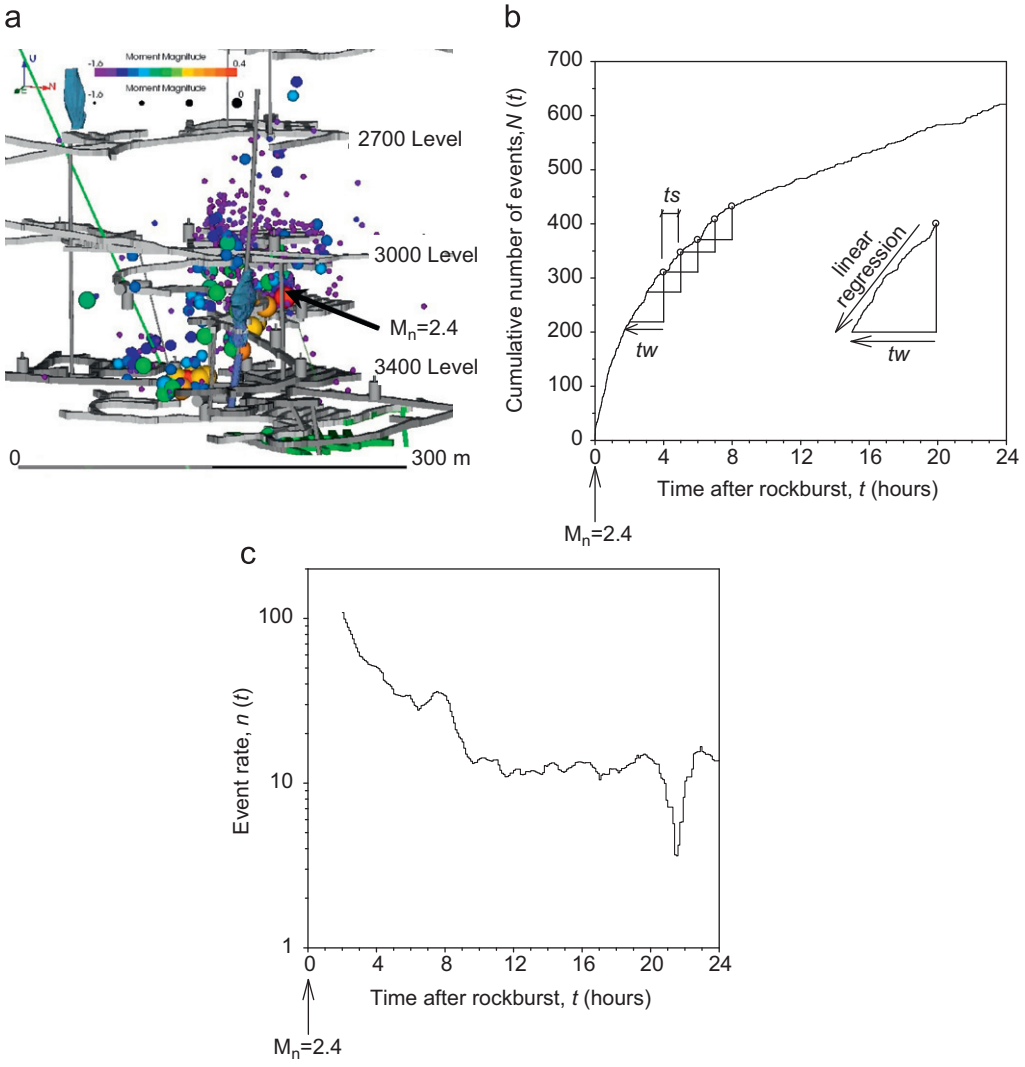

Fig. 1. Example of increased levels of seismicity following a $M_n=2.4$ rockburst at the 100/900 orebodies at the Copper Cliff North Mine. Spatial distribution of seismic events in the affected zone (frame a). Cumulative number of events and illustration of the regression time window technique (frame b) used to estimate the event rate (frame c) after the main event. A 2 h time window (*tw*) and a 0.1 h time shift (*ts*) was used to evaluate the event rate.

2. Data and methods

2.1. Sources of data

Mainly seismic data from two mining sites: Creighton and Macassa, is used throughout this paper. In the following sections, a brief description of the microseismic monitoring systems, mining method and geology of each site is provided.

2.1.1. Creighton, Sudbury. Creighton deep.

Creighton mine is located on the southern rim of the Sudbury Igneous complex. The orebodies at Creighton mine are of the contact, footwall and offset deposits and are characterized by a number of late-stage faults and shear zones. The ore is typically mined using a slot-slash mining method with pillarless, top-down and center-out mining sequence. The stopes are backfilled with cemented paste fill. The study region corresponds to the Creighton Deep, between the 6600 and 7800 levels (between 1828 and 2377 meters below surface). The underground microseismic monitoring system covering this area consists of 24 uniaxial and seven triaxial accelerometers. During the study period (January–December of 2008) a total of 26,176 microseismic events were located within this volume with moment magnitudes between -2.8 and 0.9, with the highest frequency of events occurring at the magnitude bin of -1.5 (Fig. 2a).

2.1.2. Macassa, Kirkland lake. 5036 Longhole stopes.

The mining block under study is composed of a set of primary, longitudinal, continuous retreat sublevel longhole stopes with delayed paste backfill at a depth below surface of 1500 m. The underground microseismic monitoring system surrounding the zone consists of a dense array of 66 uniaxial accelerometers. The volume of interest consists of approximately 150 m × 100 m × 100 m. During the study period (December 2004–May 2007) a total of 10,351 microseismic events were located within this volume with moment magnitudes between -1.7 and 0.7, with the highest frequency of events occurring at the magnitude bin of -1.2 (Fig. 2b). The geotechnical domains include very brittle, massive, high-strength tuff rocks in the hangingwall and massive-to-moderately jointed high strength orebody in a series of sub-parallel faults striking northeast, which dip steeply ($\sim 70^\circ$) to the south. The footwall consists of a medium-strength blocky basic syenite. Stope dimensions are approximately 3 m in thickness and 30 m width. The dominant geological structure of the zone is a single major fault intersecting the stopes,

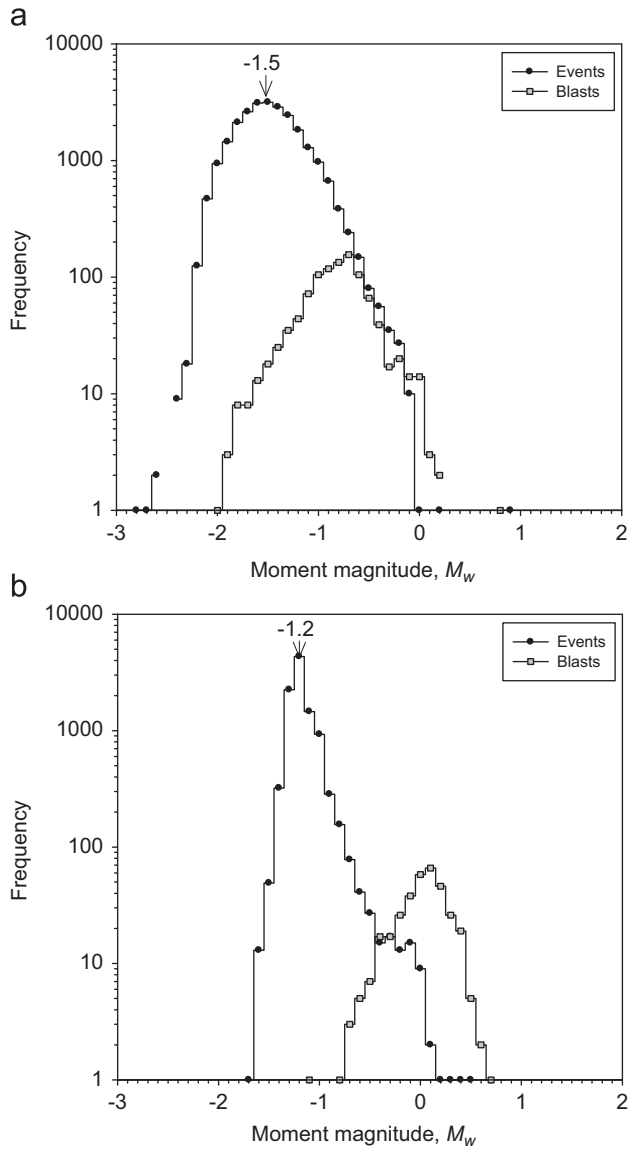

Fig. 2. Non-cumulative frequency–moment magnitude distributions for the recorded microseismic events and blasts during 2008 at Creighton Deep (frame a) and from December 2004 to May 2007 at the Macassa-5036 Longhole stopes mining zone (frame b). The magnitude bin with the highest frequency of events is indicated with an arrow.

which can be parallel to the hangingwall or footwall contact or be the actual contact itself. Inclusions are infrequent and discontinuous.

2.2. Identification of seismic sequences and magnitude filtering

There is no standard definition of aftershocks, but several are used for specific purposes [7–14]. Molchan and Dmitrieva [15] argue that aftershock identification depends on the research goals. Our principal objective is to reflect current re-entry practices where the seismic data is used for re-entry protocol decision-making in a specified volume without any formal consideration of the spatial distribution of seismicity [5] and [16]. Therefore, the analysis is relaxed to the temporal identification of seismic sequences without spatial dependence.

For a specified zone or target volume, seismic sequences are identified in time by the following approaches. The first involves using the identification provided by the mine personnel. When this identification is not available or reliable, the start of a sequence is identified by the ratios method [17]. This method evaluates the ratio $r_{N_B-N_A}=T_{N_A}/T_{N_B}$, where T_{N_A} and T_{N_B} are the time of occurrence of the N_A^{th} and N_B^{th} event following and preceding the principal event, respectively. The beginning of the sequence is identified if $r_{N_B-N_A}$ is smaller than a critical value $r^c_{N_B-N_A}$ generated by a Poisson process with a certain probability. For our analysis, we set $N_A=1$, $N_B=5$ with a probability of 1%, giving a critical value of $r^c_{5-1}=0.002$ [17]. We define the start of the seismic sequence if $r_{5-1}\le r^c_{5-1}$ for a group of at least three consecutive events. The first event of this group is identified as the principal event of the sequence regardless of its magnitude.

Note that the objective of this scheme is to identify in time, within a specified volume, the beginning of a seismic sequence based on spikes of event rate (Fig. 3) and does not attempt to classify events as foreshocks or aftershocks. Also no restriction is applied to the magnitude of the aftershocks to be less than the first event in the sequence.

After the seismic sequences were identified, a cut-off magnitude M_c filter, selected at the magnitude bin with the highest frequency of events in a non-cumulative frequency-magnitude distribution [18] and [19], was applied. The effect of this filter is to provide some degree of uniformity to the data as events below this magnitude level may not be fully recorded by the microseismic monitoring system.

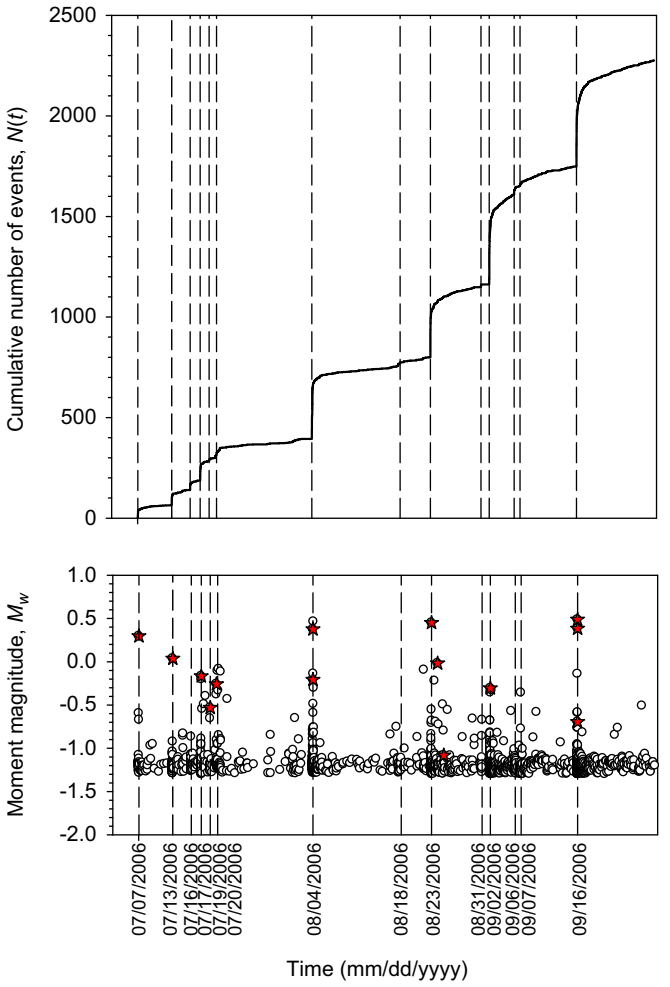

Fig. 3. Example of the seismic sequences identified by the ratios method for a time period of two months at the Macassa-5036 Longhole stopes (events labeled as blasts are identified by stars).

3. Background levels of seismicity rate

Currently there is no recognized method to decide when mining seismicity is at background levels and practices vary across the industry. The most common approach is to set maximum and minimum mine-wide background levels [6]. For the minimum level, a maintenance shutdown period with no mining activities is used, which has resulted in extremely long re-entry times. For the maximum level, data is used from specific days in which no anomalous seismic events or large crown blasts occurred. Based on a superposition of seismicity on a 24-h chart a practical method for estimating an upper bound of normal levels of seismic activity was provided [5]. In the crustal seismology literature several methods are used to define background levels as the independent temporal component, which yields the time series similar to a Poisson process [20] and [21]. The resulting seismicity levels using these methods can be substantially low for re-entry purposes [5].

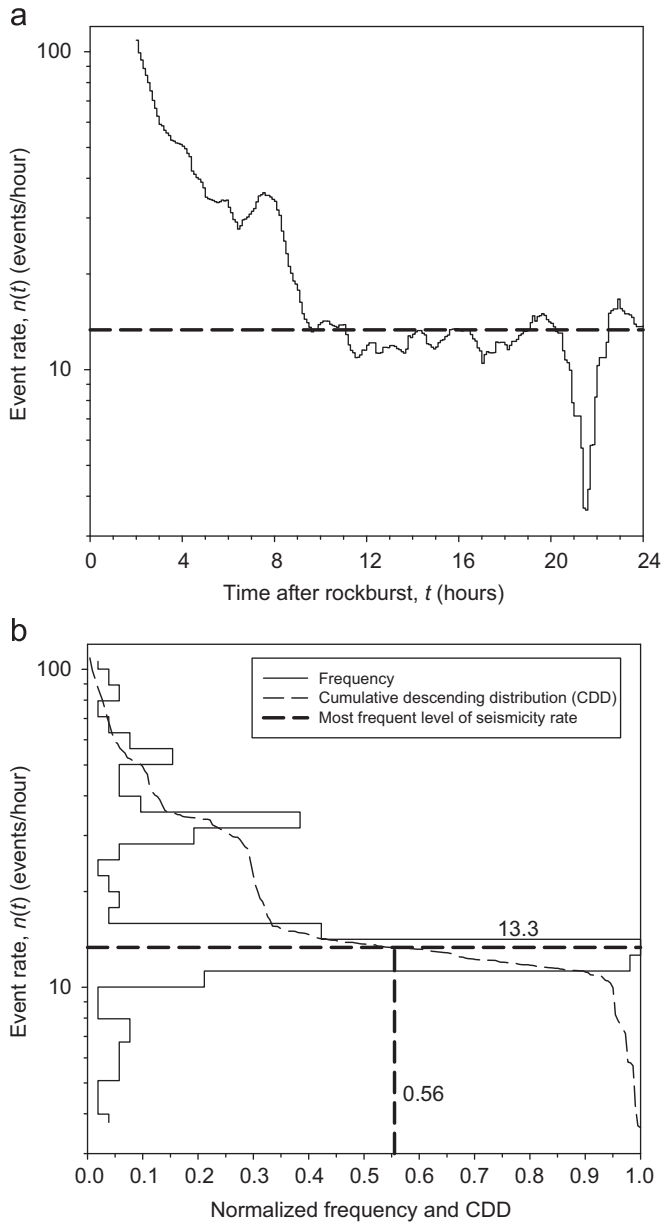

Fig. 4. Event count rate time sequence after a rockburst (frame a), and the corresponding rate histogram and cumulative descending distribution (CDD) (frame b). A 2 h time window with a 0.1 h time shift was used to evaluate the event rate.

The proposed technique is justified using rate histograms. Instead of subjectively selecting individual days for defining normal levels, the seismicity rate is continuously evaluated for the time period and volume of interest using a time window regression technique coincident with the one used for re-entry purposes. Current re-entry practices indicate that the most common regression window is 2 h [5]. To illustrate the technique, Fig. 4a presents the resulting event rate time series after an $M_n=2.4$ rockburst. In this case an approximately constant level between hours 11.2 and 20.3 is observed, indicating that most of the physical readjustments imposed by the rockburst have been released during the first 12 h. We suggest the use of this approximately constant level as representative of the background levels for re-entry protocol development. Note that rigorously speaking the decay still continues during this approximately constant level, but as observed in Fig. 4a there is no reason for delaying re-entry as the maximum change in rate has already occurred and it may take several hours to achieve a stable lower level of seismicity rate. Using the rate time sequence, the rate histogram and cumulative descending distributions (CDD) are built (Fig. 4b). To represent the rate histogram the data was divided into logarithmic intervals of 0.05. Note that the rate histogram and the CDD are normalized by the most frequent level of seismicity rate and by the total population, respectively, so they both take values from zero to one. For this particular seismic sequence the seismicity rate distributions (Fig. 4b) presents a bimodal feature; however, a pronounced most repeated level of occurrence of seismicity rate in time is observed, coincident with the approximately constant rate level previously identified in Fig. 4a.

The proposed method can be applied to any regressed seismic source parameter of interest and for any particular time period or target volume. This approach is used in Section 5 to define background levels for the entire available seismicity catalog at the two sites under study and for back-analysis of isolated seismic sequences at different mine sites.

4. Theoretical framework relating the productivity of seismicity and decay time

In this section we propose a theoretical development to demonstrate the link between the productivity of seismicity and decay time to background levels. Generally, the time decay of aftershocks is represented by the modified Omori's law. Statistical evidence for the validity of this law applied to mining seismicity and preliminary guidelines on how to use it for re-entry protocol development were proposed [16] and [22]. A generic decay-law formula can be formulated by

$$r(t)=\frac{d\Omega}{dt}=\frac{K}{(c+t)^p} \tag{1}$$

where $r(t)$ is the rate at time t measured from the principal event, Ω is the accumulated seismic quantity of interest until time t, and K, c and p are adjustable parameters. The productivity of seismicity Ω can be conveniently expressed as a function of the seismic moments at each Nth event after time zero by

$$\Omega=\sum_{i=1}^{N}(M_{o_i})^{\xi} \tag{2}$$

where $(M_{o_i})^{\xi}$ is the i^{th} seismic moment after time zero for $\xi=1$, event count for $\xi=0$ referred to as the modified Omori's law, and similar to Benioff strain [23] for $\xi=0.5$, known in the mining industry as seismic work [24]. Values of $\xi=1$ and $\xi=0$ give

dominating weights to the largest and smallest events within the analysis, respectively, while fractional values of ξ provide filters that modify the relative contributions of events in different magnitude ranges [25].

From Eq. (1) the predicted cumulative seismic quantity on a time interval $[T_A,T_B]$ is given by

$$\Omega_{T_A-T_B}=\int_{T_A}^{T_B} r(t)dt=\begin{cases} K\{\ln(c+T_B)-\ln(c+T_A)\} & \text{for } p=1 \\ K\{(c+T_B)^{1-p}-(c+T_A)^{1-p}\}/(1-p) & \text{for } p\neq 1 \end{cases} \tag{3}$$

From Eq. (3) the parameter K can be related to the total measured cumulative seismic quantity on a time interval $[T_A,T_B]$ and the other two parameters c and p by

$$K=f(T_A,T_B,c,p)\Omega_{T_A-T_B} \tag{4}$$

with

$$f(T_A,T_B,c,p)=\begin{cases} \frac{1}{\ln(c+T_B)-\ln(c+T_A)} & \text{for } p=1 \\ \frac{(1-p)}{(c+T_B)^{1-p}-(c+T_A)^{1-p}} & \text{for } p\neq 1 \end{cases} \tag{5}$$

Eq. (4) suggests that the parameter K is in direct proportion to $\Omega_{T_A-T_B}$. This is confirmed in Fig. 5 for the case of event count ($\xi=0$) where the parameter K is plotted as a function of the measured number of events N for 252 mining-induced seismic sequences from 7 different mines sites in Ontario, Canada analyzed by [16] and [22]. The parameters K, c, and p for these sequences were estimated by maximum likelihood [26] for the time interval where Eq. (1) statistically satisfies power-law decay, i.e., $c=0$. The implication of the average correlation between K and N observed in Fig. 5, for a variety of T_A, T_B and p values, is that for practical purposes the function $f(T_A,T_B,c,p)$ can be considered as a constant, and therefore the parameter K is proportional to $\Omega_{T_A-T_B}$.

Eq. (1) can also be used to estimate the time required for the seismic sequence to decay to some predefined background level of seismicity rate B

$$t_B^d=\left(\frac{K}{B}\right)^{1/p}-c \tag{6}$$

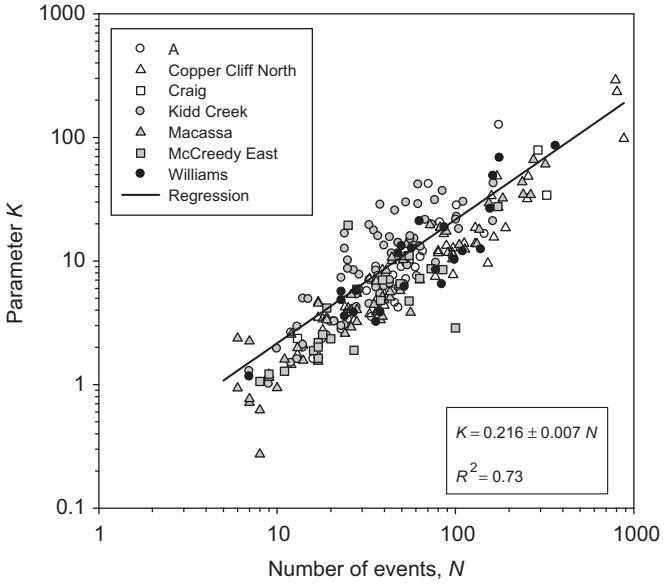

Fig. 5. Correlation between the estimated parameter K and the measured number of events N for the time interval of power-law decay for 252 mining-induced seismic sequences from 7 different mines sites in Ontario, Canada.

Eq. (6) indicates that a seismic sequence with a higher K value will result in a longer decay time to reach a certain level of seismicity rate B for given values of p and c. Note that the correlation between t_B^d and K is not necessarily linear and will depend on the average p value of the zone under study.

The analysis reveals that if a correlation can be established between a physical process and the productivity of seismicity in a given seismic environment, then a similar correlation between the decay time and the physical process should be expected. In the next Section, this will be demonstrated using case histories.

5. Case histories

5.1. Volume of mined rock

The dependency between seismic activity and the volume of extracted rock has long been recognized from theory and observations [27–30]. These models state that when a volume of rock V_m is removed at time t_0 the cumulative seismic moment released in a specific volume and within a given period of time is proportional to V_m

$$\sum_{i=0}^{N} M_{o_i}=\theta V_m \tag{7}$$

Note the similarity of Eq. (7) with Eq. (2) for $\xi=1$. The only difference is that in the decay-law formulas the main event is not considered as part of the sequence. The reason why the main event is used in Eq. (7) is that this equation is evaluated continuously in time, while for re-entry purposes the time zero is set at the time of the main event to start the analysis. We found that inclusion of the main event or not in Eq. (7) affects only the constant of proportionality θ, so in general both definitions are applicable.

The case history presented in this section corresponds to Macassa mine 5036 Longhole stopes. The mining sequence, the identified seismic sequences with their associated cumulative seismic moment for a 24 h period after the principal event, and the corresponding volume of mined rock for each mining step, are indicated in Fig. 6. Given the availability of sufficiently detailed data for this case study, the validity of relationship (7) is tested. Fig. 7a presents the cumulative seismic moment as a function of the mined volume. An overall linear correlation between the two parameters can be recognized, with the average release of seismic moment in the zone increasing at a rate of approximately $44\pm4\times10^6$ (Nm/ton). This correlation, between the seismic moment release and mined volume, and Eq. (4) indicates that the parameter K must also be proportional to the mined volume and that, in general, the time for a seismic sequence to decay to a certain level of seismic moment rate should increase as the volume of extracted rock increases.

Next, the decay time to a predefined rate level is estimated and correlated with the volume of mined rock. The most frequent level of seismic moment rate B_{SM} was established for the complete available seismic catalog and used to estimate the decay time after each mining step using a 2 h regression window and 0.1 h shift. Fig. 7b presents the seismic moment decay times $t_{B_{SM}}^d$ as a function of the mined volume in the zone. There is no improvement in the fit by assuming a power-law compared to the linear fit (Fig. 7b). Therefore, a linear increase in the decay time of approximate 0.011 (h/ton) is observed.

Note that the above analysis is simplified and there is a possible interaction of induced stresses between stopes that we have not included in the analysis. Also, the response of each stope may be affected by the fault crossing the zone. However, if the

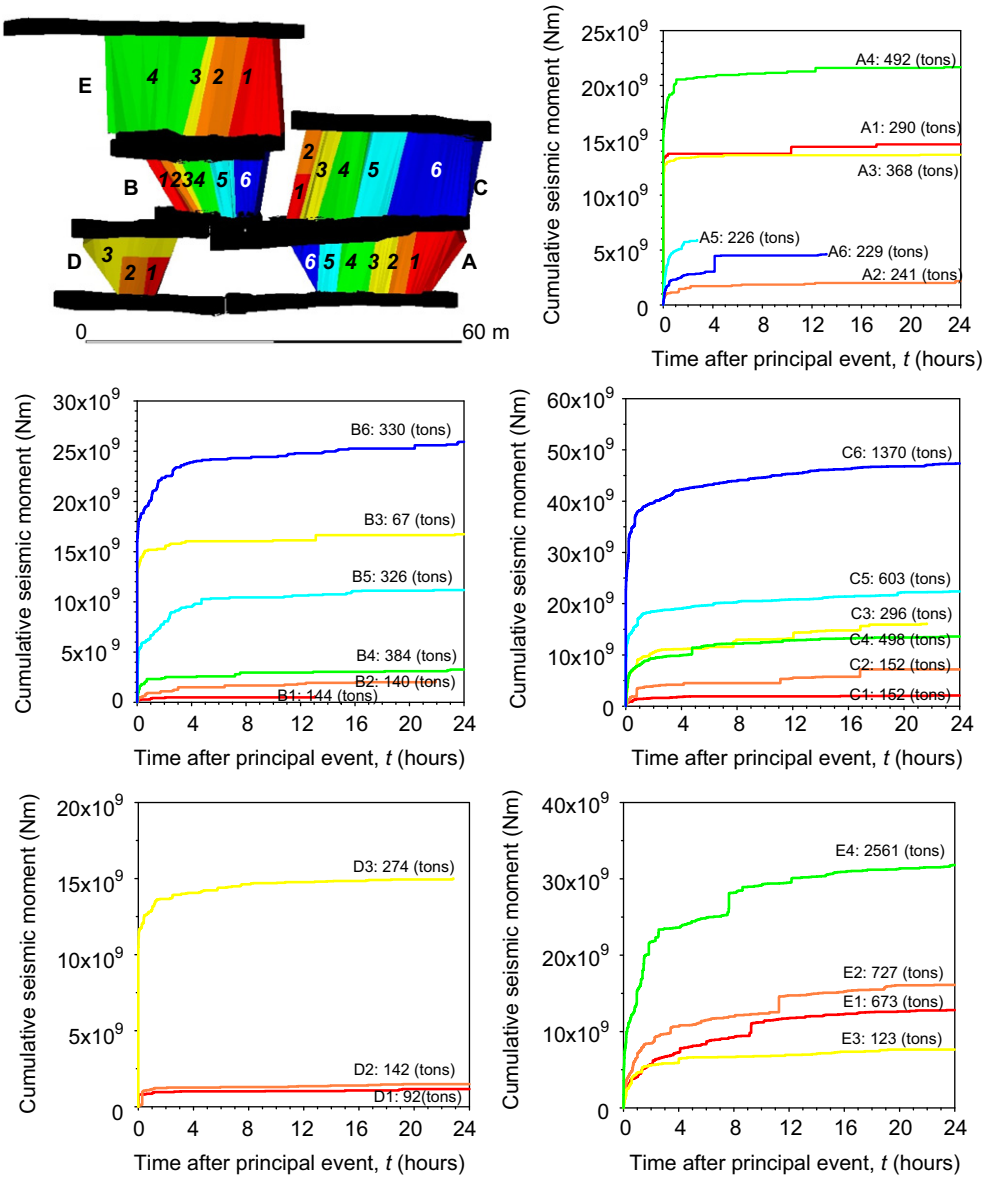

Fig. 6. Mining sequences and cumulative seismic moment for a 24 h time period after the identified principal events at the Macassa-5036 longholes stopes. The mined volume is indicated for each mining step and seismic sequence.

correlation between decay time and mined volume is tracked and updated continuously as mining progresses it could be used to estimate in advance the decay time of the rock mass for a new mining step.

5.2. Depth

Although there is considerable scatter in the measured in-situ stress databases at any given depth, a linear or exponential model is generally assumed as a best fit trend [31]. It is expected, therefore, that an increase in mining depth will result in an increase in the magnitude and frequency of mining seismicity [32,33]. Fig. 8 presents the distribution of mining seismicity as a function of depth for different moment magnitude (M_w) levels at Creighton Deep. It is seen that under the current mining scale and conditions, there is an exponential increase in the frequency of mining events for almost all magnitude bands. Also, larger microseismic events seem to occur in the deepest part of the orebody. As a reference the best fit line is shown for events with $M_w \geq -1.6$. This correlation, between the total number of microseismic events and depth, and the theoretical development presented in Section 4 may suggest that as mining progresses to deeper levels the time for a seismic sequence to decay to background levels will increase. Based on these observations the decay time of seismic work as a function of depth was evaluated. First, the most frequent level of seismic work rate B_{SW} was evaluated for the entire seismic catalog using a 2 h regression window and 0.1 h shift. Next, the identification of seismic sequences provided by the mine personnel was used. For each sequence the location of the principal event was considered as representative of the depth of the sequence. The estimated decay time to reach B_{SW} after each principal event are presented in Fig. 9 as a function of depth. The identification of the type of principal event (reported or blast) was obtained from the mine database, where reportable incidents are defined as seismic events that are felt on surface or underground and are also typically recorded by the on-site strong ground motion seismic system. Inspection of Fig. 9 provides the following:

1. The longest two decay times correspond to reported incidents.
2. There are few cases (10%) with decay times longer than 8 h.

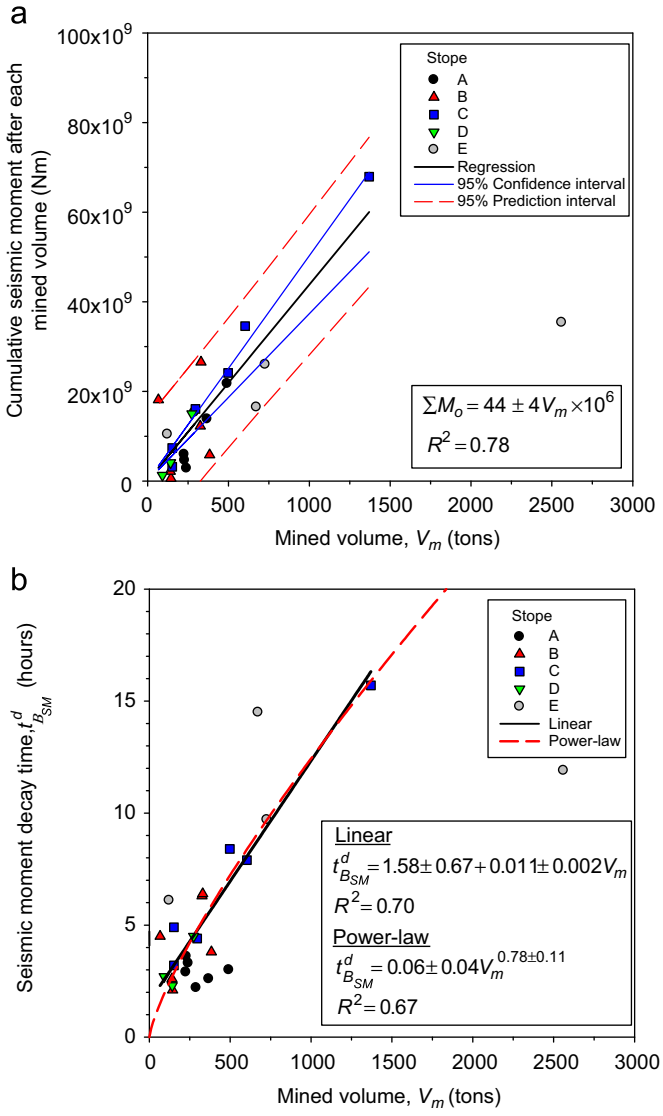

Fig. 7. (a) Total seismic moment after each mining step as a function of the volume of mined rock. (b) Seismic moment decay time as a function of the volume of mined rock.

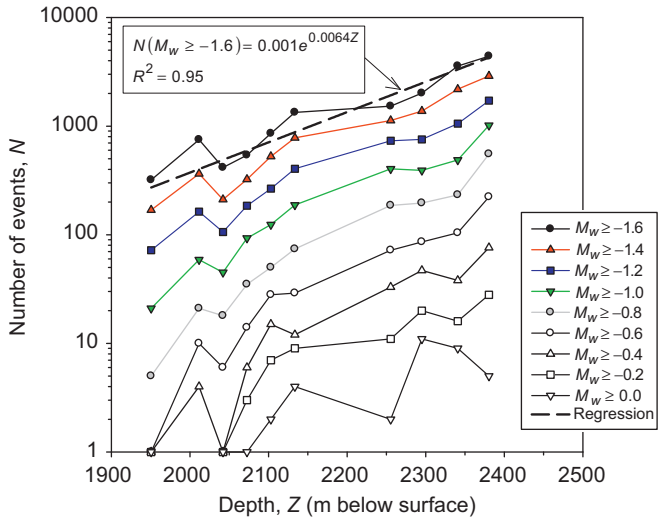

Fig. 8. Distribution of mining seismicity as a function of depth for different moment magnitude levels at Creighton Deep.

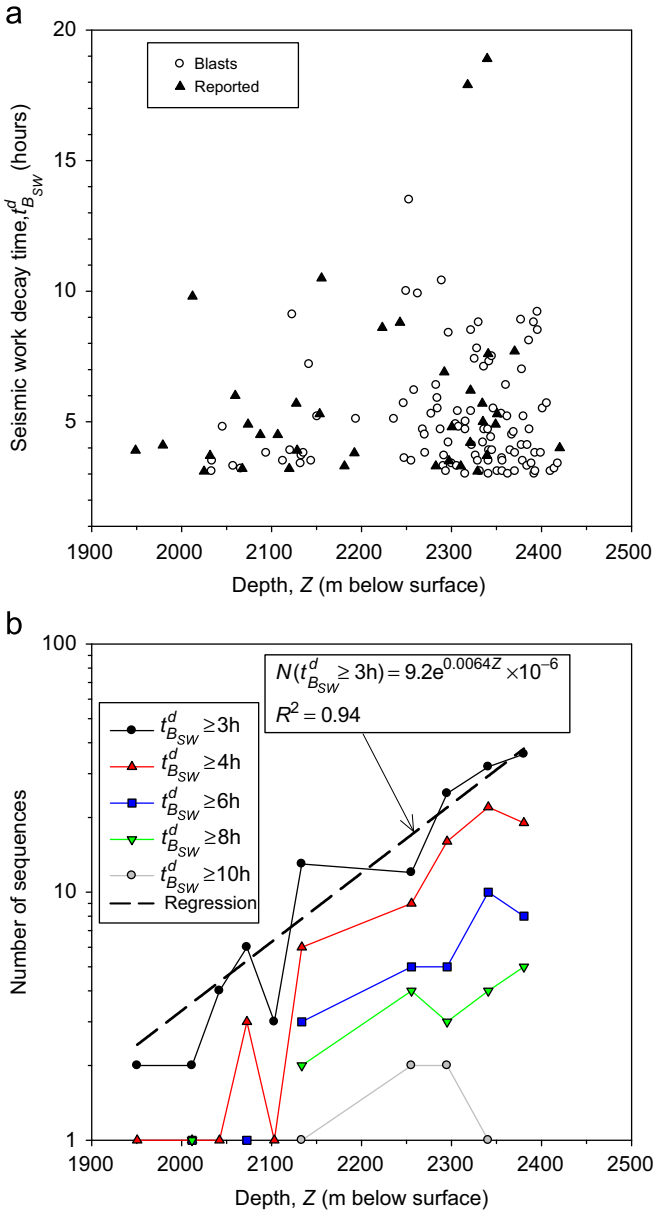

Fig. 9. Seismic work decay time as a function of depth (frame a) and distribution of seismic work decay time as a function of depth (frame b).

3. Decay times longer than 10 h only occur at depths greater than 2100 m.
4. The distribution of the decay time (Fig. 9b) increases exponentially with depth with the same proportional constant of the distribution of microseismicty with depth (Fig. 8).

This dependence with depth indicates that as the in-situ stresses increase, and for sustained mining conditions, the rock mass will take more time to respond to a new mining configuration.

5.3. *Ontario large magnitude event database*

To provide some guidance on the possible decay time and exclusion zone size after large magnitude events, data was collected from several mine-wide rockbursts and large magnitude events at different sites in Ontario. Table 1 presents the cases collected so far together with some of their characteristics, including: Nuttli (M_n) magnitude scale, date, total duration of

the sequence t_N determined by the ratios method, and the total number of events N associated with each sequence. In this paper, the Nuttli (M_n) scale is used to express the magnitude of large seismic events for mines in the Canadian Shield. Over the range of primary interest in mine seismicity (M_L=1.5–4.0), the M_n scale records magnitudes about 0.3–0.6 units greater than the M_L scale [34]. In the following, all microseismic events regardless of location error, number of sensors used in the location and moment magnitude are used for the analysis.

First, the decay time of the sequences is analyzed. In order to compare the decay times of different sites it is necessary to use a normalized and uniform criterion independent of the site specific nature of seismicity. A common most frequent level of seismicity rate may not exist for all the sites. Therefore, individual rate-histogram plots were examined for each seismic sequence, and the most frequent level of event count rate B_{EC} was determined. The resulting values are included as a reference in Table 1. The decay time $t^d_{B_{EC}}$ is defined as the time to decay to this individual most frequent level of event count rate. An example of this application was already presented in Fig. 4. The premise behind this methodology is that seismic sequences in different seismic environments have their own delay time of significant readjustment indicated by the beginning of the most frequent level of seismicity rate. Using this criterion the back-analysis of the seismic sequences was performed.

Once the decay time was estimated the spatial extent of the events was analyzed. For simplicity, the exclusion zone is represented by a sphere. In some cases, we found that the first event in the sequence was not necessarily associated with the cluster of seismicity. Considering that this can be attributed to an unusual location of the selected first event, the centroid of seismicity occurring during the first hour after the principal event was used as the center of the sphere. This point ensured a better statistical representation of the size of the affected zone. The best fit spherical radius was estimated by least squares using only events that occurred before the decay of the sequence to the most frequent level of seismicity rate. This ensures that only events associated to the maximum change in rate of the sequence are included in the exclusion zone.

Fig. 10 presents the resulting decay times for the event count parameter and the best fit spherical radius as a function of the Nuttli magnitude for the 22 sequences analyzed. Despite some natural dispersion in the data, a remarkable and significant exponential increase in the decay time and the spherical radius representing the exclusion zone can be recognized as the Nuttli magnitude of the event increases.

Table 1
List of analyzed sesimic sequences following large magnitude events and rockbursts from Ontario mines.

#	Site	Date (mm/dd/yyyy)	M_n	t_N (h)	N	B_{EC} (events/h)
1	A	10/13/2006	1.1	27.3	48	2.8
2	Copper Cliff North	09/30/2004	1.9	25.6	51	2.8
3	Copper Cliff North	11/30/2004	2.4	29.9	855	4.5
4	Copper Cliff North	06/10/2005	2.1	10.3	172	7.1
5	Copper Cliff North	06/11/2006	2.8	72.1	1880	14.1
6	Copper Cliff North	09/24/2008	2.4	69.4	164	17.8
7	Copper Cliff North	09/11/2008	3.8	165.6	1411	4.5
8	Craig	06/22/2007	2.2	37.5	507	11.2
9	Creighton	11/29/2006	4.1	165.5	3742	11.2
10	Creighton	06/15/2007	3.0	27.6	591	11.2
11	Creighton	10/07/2007	3.1	53.6	801	8.9
12	Creighton	10/17/2007	1.0	18.4	86	4.5
13	Creighton	11/20/2007	0.6	9.3	24	2.8
14	Creighton	02/07/2008	2.4	45.9	197	3.5
15	Creighton	04/17/2008	1.5	7.1	23	1.8
16	Creighton	12/06/2008	2.9	25.3	161	5.6
17	Creighton	03/14/2009	2.6	197.7	2933	5.6
18	Fraser	10/16/2008	2.4	14.0	86	3.5
19	Garson	12/05/2008	3.3	14.4	117	5.6
20	Kidd Creek	03/02/2006	1.6	23.5	223	2.8
21	Kidd Creek	01/06/2009	3.8	71.6	116	2.8
22	Macassa	07/12/2008	3.1	469.7	583	1.8

6. Discussion

The definition of background levels of seismicity rate based on selection of single days may not be completely representative of a common process in time in a given seismic environment. A procedure for estimating seismicity rate thresholds for re-entry protocol development was proposed. This technique is based on the physical concept that the most frequent level of seismicity

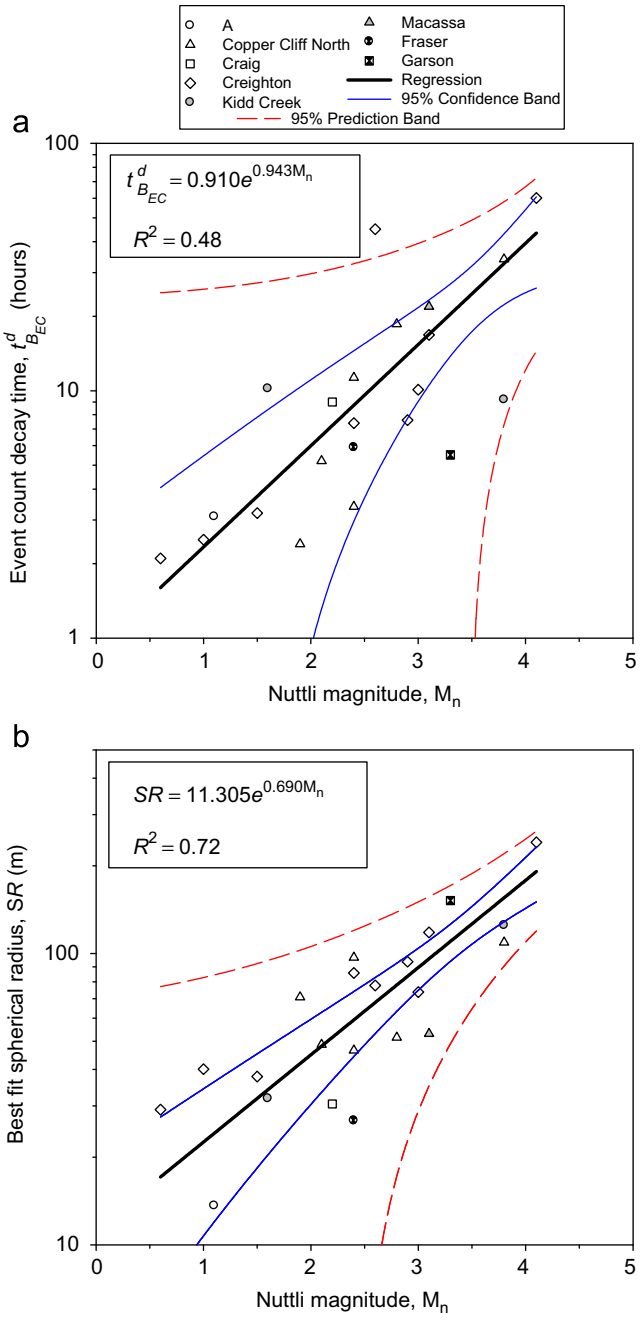

Fig. 10. Event count decay times (frame a) and best fit spherical radius (frame b) as a function of the Nuttli magnitude for different seismic sequences in Ontario mines.

rate is the state in which the rock mass is most likely to be most of the time, and that blasts and large magnitude events disrupt this equilibrium. This is a major improvement in the standardization and development of re-entry protocols. It can be applied to a complete catalog for evaluating the global response of the seismic environment or to isolated seismic sequences for back-analysis. There is also almost no need for interpretation, as the most frequent level is selected automatically by the scheme.

Three case histories were reviewed, selected to illustrate the possible effects of factors such as: volume of mined rock, depth, and magnitude of large events, on the decay time of mining-induced seismic sequences.

A significant positive linear correlation was established between the volume of mined rock and the decay time of seismic moment. This correlation is an effect of the influence of stress changes resulting from stope enlargement during blasting. By using this correlation it is possible to estimate in advance the decay time response of the rock mass to a new mining configuration. This can be particularly usefully for developing a proactive re-entry protocol that can be adjusted as new data becomes available.

Using data from the Creighton Mine, microseismicity was shown to correlate with depth. An exponential increase in the frequency of mining seismic events for almost all magnitude bands was observed. As mining progresses to deeper levels, and for a sustained mining condition, a larger number of seismic sequences with longer decay times are found. This is a direct consequence of the in-situ stresses that increase with depth.

Preliminary correlations for estimating the decay time and size of the exclusion zone based on the Nuttli magnitude of the main event were proposed. This is a major development for mines with less experience, developing their first re-entry protocol, and for areas with poor coverage of the microseismic monitoring system. The dispersion in Fig. 10 not only reflects the site specific nature of seismicity but also suggests that the mechanism of the sequence may play a role in determination of the decay time. It is expected that for mining-induced seismic sequences, the mechanism involved (e.g., pillar burst, fault slip, strain burst) may play a role in the aftershock productivity. This has been accounted for in the crustal literature by considering aftershock statistics separately for intraplate [35] and interplate [36] earthquakes. The database of seismic sequences following large magnitude events from Ontario mines needs to be extended, in terms of both information on currently included cases and addition of more cases. A more refined classification of the cases with respect to mining factors may help to introduce the mechanism in the proposed correlations. Based on the results of a re-entry protocol survey [5], some mines were using a spherical radius to restrict access. Distances of less than 50 m were related mostly to strain burst damage and entry mining methods, while distances between 50 and 100 m included open stope mining. Distances larger than 100 m were associated with regional fault slip in certain mines. Inspection of the average correlation determined in Fig. 10b indicates that distances less than 50 m are found for $M_n \leq 2.2$, while distances over 100 and 200 m are associated with $M_n \geq 3.2$ and $M_n \geq 4.1$, respectively. The proposed correlation between exclusion zone and magnitude of the main event corresponds very well with the identified ranges of exclusion zones currently used at the surveyed mines and with previous rockburst classifications systems [37].

7. Conclusions

A method for quantifying background levels of seismicity rate for re-entry protocol development using analysis of standard mining seismic databases was presented. When applied to the case studies reported here, it was shown to produce useable relations for management of seismic risk related to large magnitude events/rockbursts or blasts. This successful demonstration suggests the potential usefulness of the method as a framework for evaluating background levels for re-entry protocol development.

Case histories relating the decay of seismicity with mining activities on the basis of a theoretical framework were presented. These correlations are not intended to replace real-time data analysis. They were developed to quantify and reflect the site specific influence of diverse mining factors on the decay time response of the rock mass. However, the presented methodology should be widely applicable.

Several controlling parameters in the decay time of mining-induced seismic sequences were presented, such as: volume of mined rock, depth and magnitude of main event; however, there is insufficient data to rank their relative importance and provide a methodology of how to account for these factors for a general re-entry protocol. It is suggested that this could be a productive area for further investigation.

Acknowledgments

We would like to thank Dave Collins and one anonymous referee for their critical reviews, which led to improvements in the manuscript. This research was supported by a grant from the Workplace Safety and Insurance Board (WSIB) of Ontario. The authors wish to acknowledge the permission of the mines studied to publish this work.

References

[1] Omori F. On the after-shocks of earthquakes. J Coll Sci, Imp Univ Tokyo 1894;7:111–200.
[2] Utsu T. A statistical study of the occurrences of aftershocks. Geophys Mag 1961;30:521–605.
[3] Utsu T, Ogata Y, Matsu'ura R. The centenary of the Omori formula for a decay law of aftershocks activity. J Phys Earth 1995;43:1–33.
[4] Shcherbakov R, Turcotte DL, Rundle JB. Aftershock statistics. Pure Appl Geophys 2005;162:1051–76.
[5] Vallejos JA, McKinnon SD. Guidelines for development of re-entry protocols in seismically active mines. In: Proceeding of the 42nd US Rock mechanics symposium, San Francisco, California, ARMA/USRMS, 2008, paper 08-97.
[6] Malek F, Leslie IS. Using seismic data for rockburst re-entry protocol at Inco's Copper Cliff North mine. In: Proceedings of the 41st US rock mechanics symposium, Golden, Colorado, ARMA/USRMS, 2006, paper 06-1163.
[7] Isacks BL, Sykes LR, Oliver J. Spatial and temporal clustering of deep and shallow earthquakes in the Fiji–Tonga–Kermadec region. Bull Seism Soc of Am 1967;57:935–58.
[8] Shlien S, Toksoz MN. A statistical method of identifying dependent events and earthquake aftershocks. Earthquake Notes 1974;45:3–16.
[9] Kagan YY, Knopoff L. Statistical search for non-random features of the seismicity of strong earthquakes. Phys Earth Plan Int 1976;12:291–318.
[10] Reasenberg P. Second-order moment of central California seismicity, 1969–1982. J Geophy Res 1985;90:5479–95.
[11] Ogata Y. Statistical models for earthquake occurrences and residual analysis for point processes. J Am Stat Assoc 1988;83:9–27.
[12] Davis SD, Frohlich C. Single-link cluster analysis, synthetic earthquake catalogues, and aftershock identification. Geophys J Int 1991;104:289–306.
[13] Davis SD, Frohlich C. Single-link cluster analysis of earthquake aftershocks: decay laws and regional variations. J Geophy Res 1991;96:6335–50.
[14] Kagan YY, Jackson DD. Comment on: 'Testing earthquake prediction methods: "The West Pacific short-term forecast of earthquakes with magnitude MwHRV $\geq$ 5.8"' by V.G. Kossobokov. Tectonophysics 2006;413:33–38.
[15] Molchan GM, Dmitrieva OE. Aftershock identification: methods and new approaches. Geophys J Int 1992;109:501–16.
[16] Vallejos JA, McKinnon SD. Omori's law applied to mining-induced seismicity and re-entry protocol development. Pure Appl Geophys 2010;167(1):91–106.
[17] Frohlich C, Davis S. Identification of aftershocks of deep earthquakes by a new ratios method. Geophys Res Lett 1985;12:713–6.
[18] Wiemer S, Wyss M. Minimum magnitude of complete reporting in earthquake catalogs: examples from Alaska, the Western United States, and Japan. Bull Seism Soc Am 2000;90:859–69.

[19] Woessner J, Wiemer S. Assessing the quality of earthquake catalogues: estimating the magnitude of completeness and its uncertainty. Bull Seism Soc Am 2005;95:684–98.
[20] McNally KC. Spatial, temporal and mechanic character in earthquake occurrence, a segment of the San Andreas Fault in central California, PhD dissertation, University of California, Berkeley, California; 1976.
[21] Habermann RE, Wyss M. Background seismicity rates and precursory seismic quiescence: Imperial Valley, California. Bull Seismol Soc Am 1984;74: 1743–55.
[22] Vallejos JA, McKinnon SM. Re-entry protocols for seismically active mines using statistical analysis of aftershock sequences. In: Rock engineering in difficult conditions. Proceedings of the 20th Canadian rock mechanics symposium, Toronto, Canada; 2009, paper 4028.
[23] Benioff H. Earthquakes and rock creep: (part I: creep characteristics of rocks and the origin of aftershocks). Bull Seismol Soc Am 1951;41:31–69.
[24] SeisWatch. ESG Hyperion Software User's Guide-v13.0. 2 [Chapter 4].
[25] Ben-Zion Y, Lyakhovsky V. Accelerated seismic release and related aspects of seismicity patterns on earthquake faults. Pure Appl Geophys 2002;159:2385–412.
[26] Ogata Y. Estimation of the parameters in the modified omori formula for aftershock frequencies by the maximum likelihood procedure. J Phys Earth 1983;31:115–24.
[27] McGarr A. Seismic moments and volume changes. J Geophys Res 1976;81: 1487–94.
[28] Cook NGW. Seismicity associated with mining. Eng Geol 1976;10:99–122.
[29] Glowacka E, Kijko A. Continuous evaluation of seismic hazard induced by the deposit extraction in selected coal mines. Pure Appl Geophys 1989;129: 523–33.
[30] Srinivasan C, Arora SK, Yaji RK. Use of mining and seismological parameters as premonitors of rockbursts. Int J Rock Mech Min Sci 1997;34:1001–8.
[31] Martin CD, Kaiser PK, Stress Christiansson R. instability and design of underground excavations. Int J Rock Mech Min Sci 2003;40:1027–47.
[32] Cai MF, Ji HG, Wang JA. Study of the time–space–strength relation for mining seismicity at Laohutai coal mine and its prediction. Int J Rock Mech Min Sci 2005;42:145–51.
[33] He X, Li S, Pan K, Zhang T, Wang L, Xu Z, et al. Mining seismicity, gas outburst and the significance of their relationship in the study of physics of earthquake source. Acta Seismol Sin 2007;20:332–47.
[34] Hasegawa HS, Wetmiller RJ, Gendzwill DJ. Induced seismicity in mines in Canada—an overview. Pure Appl Geophys 1989;129(3-4):423–53.
[35] Yamanaka Y, Shimazaki K. Scaling relationship between the number of aftershocks and the size of the main shock. J Phys Earth 1990;38(4):305–24.
[36] Guo Z, Ogata Y. Correlation between characteristics parameters of aftershock distribution in time, space and magnitude. Geophys Res Lett 1995;22(8): 993–6.
[37] Blake W. Hedley DGF. Rockbursts: case studies from North American hard-rock mines. Society for Mining, Metallurgy, and Exploration, Inc.; 2003.